Journal of Thermal Analysis and Calorimetry (2018) 134:1505–1519
https://doi.org/10.1007/s10973-018-7810-x

Preparation of a novel mono-component intumescent flame retardant for enhancing the flame retardancy and smoke suppression properties of epoxy resin

Long Yan[1,2] · Zhisheng Xu[1,2] · Xinghua Wang[2] · Nan Deng[1,2] · Zhiyong Chu[1,2]

Received: 24 March 2018 / Accepted: 7 October 2018 / Published online: 17 October 2018

Abstract

A novel mono-component intumescent flame retardant named pentaerythritol phosphate melamine salt (PPMS)-functionalized expandable graphite (PPMS-EG) was synthesized and carefully characterized by Fourier transform infrared spectroscopy, ^{1}H nuclear magnetic resonance spectroscopy, scanning electron microscopy (SEM)–energy-dispersive X-ray spectrometry, and thermo-gravimetric (TG) analyses. Then, PPMS-EG was incorporated into epoxy resin (EP) to enhance fire safety. The flammability properties of EP composites were investigated by limiting oxygen index (LOI), UL94 vertical burning test, and cone calorimeter test. As expected, PPMS-EG imparts good flame retardancy to epoxy resin, and EP matrix with 20 mass% PPMS-EG passes the UL94 V-0 rating and the LOI value reaches 27.3%. Cone calorimeter test shows that the incorporation of PPMS-EG dramatically reduces the heat release and smoke production of EP, and the peak heat release rate and peak smoke production rate of EP composite with 15 mass% PPMS-EG are reduced by 68.7% and 46.3%, respectively, compared to those of EP. By comparison with either PPMS or expandable graphite, the same addition of PPMS-EG produces higher flame-retardant and smoke suppression efficiencies in EP matrix due to the formation of a more compact and intumescent char layer, as determined from digital photographs and SEM images. TG results show that PPMS-EG significantly enhances the thermal stability and char-forming ability of EP composites. Char residue analysis reveals that PPMS-EG positively contributes to the formation of more phosphorus-rich cross-linking char and aromatic char in the condensed phase, thus exhibiting a more thermally stable char against the release of heat and smoke. Overall, PPMS-EG can be used as a highly efficient mono-component intumescent flame retardant for preparing super flame-retarded EP composites.

✉ Long Yan
ylong015@163.com

[1] Institute of Disaster Prevention Science and Safety Technology, Central South University, Changsha 410075, China

[2] School of Civil Engineering, Central South University, Changsha 410075, China

Graphical abstract

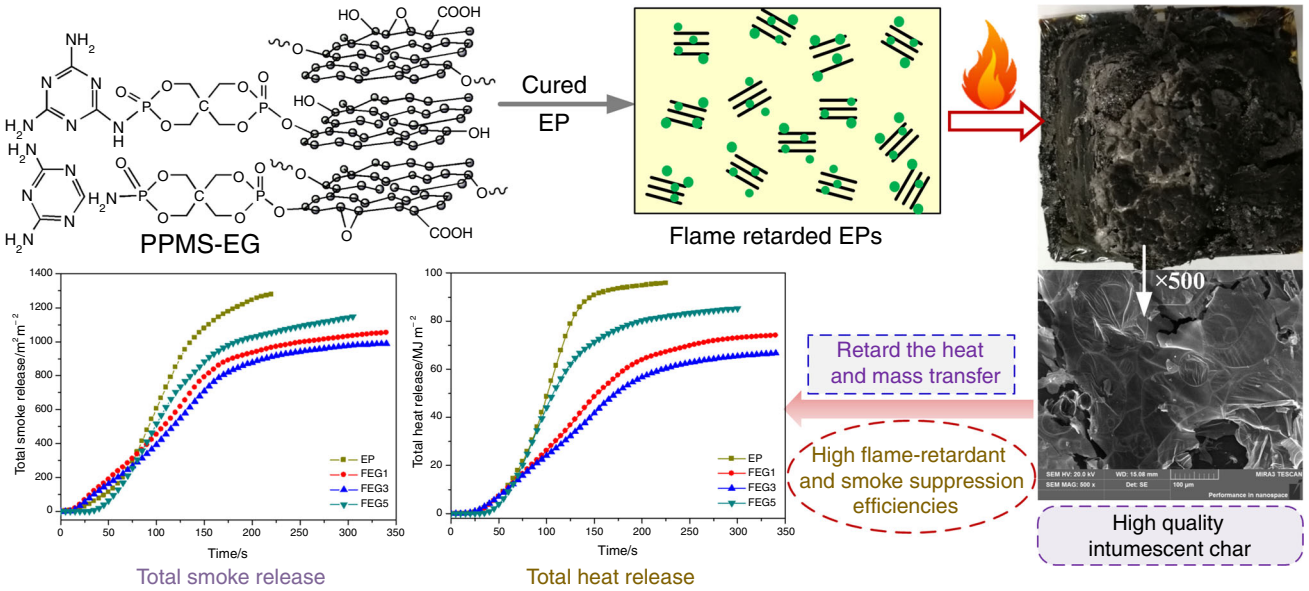

Keywords Expandable graphite · Mono-component intumescent flame retardant · Epoxy resin · Flammability · Thermal behavior

Introduction

Epoxy resin (EP) is widely applied in adhesive, coating, and composite areas due to its excellent chemical corrosion resistance, good mechanical properties, high adhesion and insulation property, and low cost [1]. However, epoxy resin will release large amounts of smoke and heat during combustion, which severely restricts its functional applications in some fields with fire safety requirement [2]. Therefore, it is imperative to reduce the flammability of epoxy resin for broadening its application. To solve this problem, many efforts focus on the development and design of flame-retarded EP with desired fire safety by incorporating appropriate flame retardants [3].

Recently, intumescent flame retardant (IFR) is considered as a promising candidate to obtain high performance of flame-retarded EP due to its excellent properties such as low smoke and toxicity, and high flame retardant efficiency [4, 5]. The intumescent flame retardants can be divided into organic IFR and inorganic IFR. For organic IFR, it mainly consists of three ingredients: an acid source (such as ammonium polyphosphate, APP), a carbon source (such as pentaerythritol, PER), and a blowing agent (such as melamine, MEL). When heated, the organic IFR formulations can swell and form an intumescent cellular charred layer on the surface, thus effectively preventing the underlying materials from the flame or heat flux [6]. However, a relatively high loading level of typical organic IFR formulation (e.g., APP–PER–MEL system) should be incorporated into the polymer matrix to satisfy the fire safety requirement due to the low flame-retardant efficiency, which will deteriorate the mechanical properties of materials [7]. To overcome this drawback, many efforts have focused on the synthesizing of melamine salt of pentaerythritol phosphate and its derivatives, which exhibited excellent flame-retardant efficiency and good compatibility in polymers due to the chemical combination of all three ingredients of an IFR formulation into a single molecule. Zhang et al. [8] synthesized a mono-component intumescent flame retardant named pentaerythritol phosphate melamine salt (PPMS) for improving the flame retardancy of ethylene–vinyl acetate copolymer (EVA). Makhlouf et al. [9] prepared a novel mono-component intumescent flame retardant, melamine salt of montmorillonite phosphate, which endowed linear low-density polyethylene with excellent flame retardancy. Zhang et al. [10] prepared benzoguanamine spirocyclic pentaerythritol bisphosphonate as mono-component intumescent flame retardant for developing modified waterborne polyurethane with super flame retardancy. Although the performance of above mono-component IFRs has been gratifying, it is still essential to improve their flame-retardant efficiency at lower loading levels. The usage of

synergistic agent in intumescent system is a highly efficient way to reduce the loading of IFR as much as possible.

Expandable graphite (EG) is a well-known inorganic intumescent flame retardant, which is widely used as a carbon char-forming agent, blowing agent, and smoke suppressant [11]. EG is a layered crystal made of successive sheets of carbon atoms tightly connected by Van der Waals forces. When exposed to heat, EG can expand and generate a voluminous insulating layer to protect the polymeric matrix from further combustion [12]. The flame-retarded effect of EG is effected by the particle size of EG, and the large size of EG usually exhibits good flame-retarded effect and high volume expansion ratio in polymers [13]. Li et al. [14] showed that the larger size of EG could effectively improve the flame-retardant properties of polyurethane foams while the smaller size of EG has no particular effect on the flame-retardant properties, which can be ascribed to that the large size of EG can form a large volume of expanded graphite and thus effectively hinder the heat penetration process during burning. Luo et al. [15] revealed that EG with large particle sizes (430 μm and 960 μm) could effectively enhance the flame-retardant properties of water-blown semirigid polyurethane foams (SPFs), while EG with small particle size of 70 μm has no effect on the fire behavior of the composite. Laachachi et al. also found that the EG with small particle size has almost no effect on the thermal degradation and combustion behavior of epoxy matrix and only acts as an inert filler in the condensed phase [16]. Although the large particle size of EG performs good flame-retarded effect, a relatively high loading level of EG is still required to acquire a satisfactory flame-retardant grade which will damage the mechanical properties of polymer matrix. In addition, the rapid reaction of EG forms an unstable char layer with insufficient adhesion which is easily destroyed by flame pressure and heat flux during combustion [17]. Therefore, it is crucial to combine EG with other flame retardants to acquire an excellent flame-retardant efficiency.

In recent years, many efforts have confirmed that the combination of inorganic EG with organic IFRs exhibited excellent synergist flame-retarded effect in a large range of polymers including high-density polyethylene/ethylene vinyl acetate copolymer [11], epoxy resin [17], nature rubber [18], rigid polyurethane foam [19], polypropylene [20], polyisocyanurate–polyurethane foam [21], polylactide [22]. The generally accepted synergistic flame-retardant mechanism between EG and organic IFR is that the strong interfacial bonding between these two different char residues originated from EG and IFR can strength the continuity and integrality of intumescent char, resulting in a stronger shield effect in condensed phase [17, 20]. However, the lack of chemical bonding between EG and organic IFR still causes a distinct interface between their respective char residues after burning, thus resulting in a negative effect on the enhancement of barrier effect in condensed phase. In order to overcome this problem, functionalized expandable graphite with organic intumescent flame retardant is one of the promising strategies to improve the interfacial adhesion of different char residues and exhibit high flame-retardant efficiency [23]. Han et al. [23] synthesized a unique hybridized intumescent flame retardant by grafting organic chains containing phosphorous and nitrogen elements on the surface of EG and applied that to develop modified cyanate ester resins with excellent flame retardancy. Chen et al. [24] revealed that functionalized EG by pentaerythritol phosphate imparted good flame retardancy and smoke suppression properties in silicone rubber composites. Although many functionalized methods have been reported, it still needs to explore more organic intumescent flame retardants to develop functionalized EG with super flame-retardant efficiency. In particular, the chemical combination of EG and pentaerythritol phosphate melamine salt into a single molecule is expected to develop a novel mono-component IFR with excellent flame-retardant efficiency, which has not been reported in the literature to the best of our knowledge.

In this paper, a novel mono-component intumescent flame retardant (PPMS-EG) was synthesized by grafting pentaerythritol phosphate melamine salt (PPMS) on the surface of EG and thoroughly characterized by FTIR, ^{1}H NMR, and TG analysis. Then, PPMS-EG was applied to develop modified epoxy resins with super flame retardancy and smoke suppression properties. The thermal behavior, flame retardancy, and smoke suppression properties of modified EPs were intensively investigated by different measurements. In addition, the morphologies and chemical structures of char residues were analyzed by FTIR, X-ray photoelectron spectroscopy (XPS), and SEM–EDS analysis, and the potential flame retardant and smoke suppression mechanism of PPMS-EG was also proposed.

Experimental

Materials

Expandable graphite (EG, purity: 99%), with an average size of 45 μm and expansion volume of 15, was obtained from Qingdao Xinghua Graphite Co., Ltd., China. Pentaerythritol (PER, purity: 95%) and melamine (MEL, purity: 99.5%) were supplied by Hangzhou JLS Flame

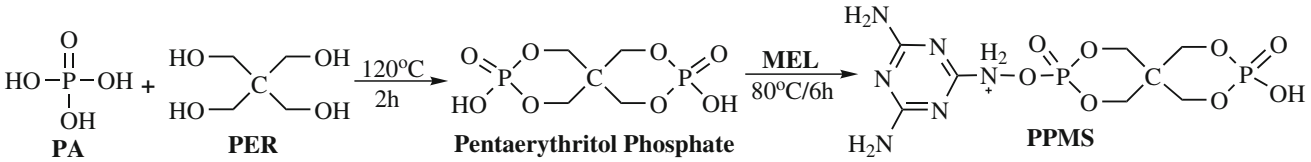

Scheme 1 Synthesis route of PPMS flame retardant

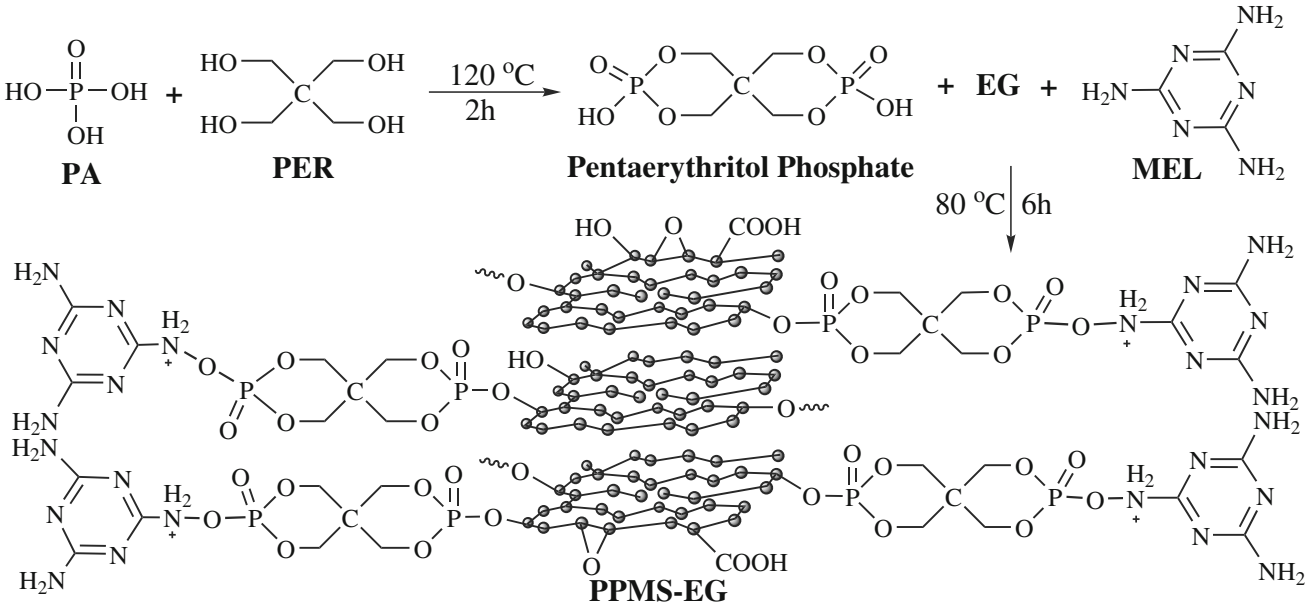

Scheme 2 Synthesis route of PPMS-EG flame retardant

Retardant Co., Ltd., China. Absolute ethyl alcohol (AR grade, 99.8%) and dimethyl-benzene (AR grade, 99.8%) were acquired from Sinopharm Chemical Reagent Co., Ltd., China. Phosphoric acid (PA) with a mass concentration of 85% was supplied by Chengdu Jinshan Chemical Reagent Co., Ltd., China. Epoxy resin (E-44, epoxy value: 0.44 mol/100 g) was supplied by Zhenjiang Danbao Resin Co., Ltd., China, and polyamide resin (low molecular 650) was used as curing agent. All the reagents were used as received without any further purification.

Synthesis of PPMS and PPMS-functionalized EG

The PPMS was synthesized according to the procedure as that previously reported [25]. Firstly, the PA (34.59 g, 0.3 mol) and PER (13.62 g, 0.1 mol) were put into a 500-mL three-neck flask and continuously stirred at 120 °C for 2 h to obtain pentaerythritol phosphate (PPS). Then, MEL (13.87 g, 0.11 mol) and 300 mL absolute ethyl alcohol (used as water-carrying agent) were added into the above PPS, and the mixture was stirred at 80 °C for 6 h to obtain crude pentaerythritol phosphate melamine salt (PPMS). Next, the crude product was cooled and filtrated

Table 1 Formulations and flammability tests of flame-retarded epoxy resins

Samples	Cured EP/mass%	PPMS/mass%	PPMS-EG/mass%	EG/mass%	LOI/%	UL94 rating
EP	100	0	0	0	19.2	HB
FEG1	85	15	0	0	22.8	V-2
FEG2	90	0	10	0	24.2	V-2
FEG3	85	0	15	0	25.8	V-1
FEG4	80	0	20	0	27.3	V-0
FEG5	85	0	0	15	25.4	HB

to remove the solvent. Finally, the white products were washed with absolute ethyl alcohol for five times and then dried overnight under vacuum at 80 °C to obtain PPMS. The synthesis route of PPMS is shown in Scheme 1.

The synthesis route of PPMS-functionalized EG (PPMS-EG) is illustrated in Scheme 2. Firstly, the mixture of PA (34.59 g, 0.3 mol) and PER (13.62 g, 0.1 mol) was reacted at 120 °C for 2 h in a 500-mL three-neck flask to obtain PPS. Then, EG (10 g), MEL (13.87 g, 0.11 mol), and 300 mL absolute ethyl alcohol were put into the above PPS with continuous stirring, and the reaction was maintained at 80 °C for 6 h to obtain the crude PPMS-EG. After that, the crude product was filtrated and washed with absolute ethyl alcohol for five times, and the black product was dried overnight under vacuum at 80 °C to obtain PPMS-EG.

Preparation of flame-retarded epoxy resins

The flame-retarded EP composites were prepared through room temperature curing process as the following steps. First, a certain mass ratio of EP and flame retardants was dissolved in dimethyl-benzene with continuous stirring by a high-speed disperser at a speed of 600 r min^{-1} until a homogeneous liquid was formed. Then, the polyamide resin was dissolved in dimethyl-benzene and then added into the EP mixture as curing agent. The mass ratio of epoxy resin to polyamide resin was 2:1. The cured EP mixture was stirred through a high-speed disperser at a speed of 600 r min^{-1} for 30 min, and the end mixtures were poured into aluminum molds with dimensions of 100 mm × 100 mm × 3 mm and cured for one week at room temperature to obtain flame-retarded EPs. The formulations and flammability tests of flame-retarded EPs are listed in Table 1, where the amount of cured EPs is equal to the sum amount of both epoxy resin and polyamide resin in flame-retarded EPs.

Characterization and measurement

Fourier transform infrared spectroscopy (FTIR) was performed on a Nicolet FTIR IS50 spectrometer (Thermo, USA) over the wavenumber range from 4000 to 500 cm^{-1} using KBr pellets. ^{1}H nuclear magnetic resonance spectroscopy (^{1}H NMR) was recorded on a Bruker AVANCE III 400-M NMR spectrometer with DMSO-d_6 as a solvent.

The morphologies of flame retardants and char residues obtained after the cone calorimeter test were investigated with a MIRA 3 LMU scanning electron microscopy (Tescan, Czech Republic) with a voltage of 20 kV. Energy-dispersive X-ray spectrometry (EDS) was used to analyze the elemental content of samples, and it was carried on an X-Max20 X-ray probe (Oxford instruments, UK) as the component of the SEM.

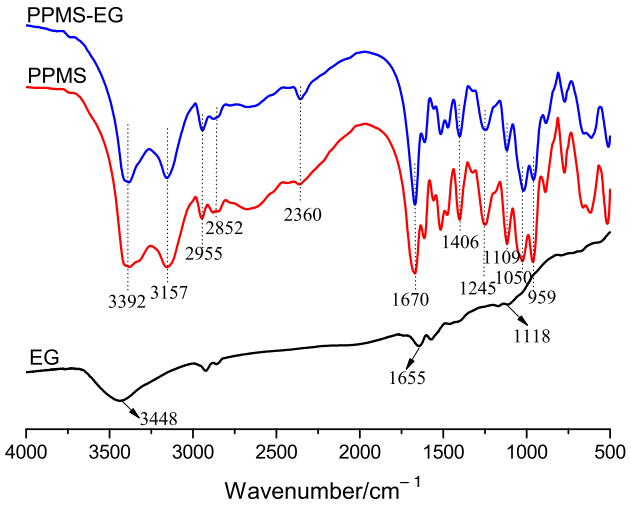

Fig. 1 FTIR spectra of EG, PPMS and PPMS-EG flame retardants

Limiting oxygen index (LOI) test was performed on a HC-2 oxygen index meter (Jiangning Analysis Instrument Company, China) according to ASTMD 2863, and the size of the samples was 100 mm × 6.5 mm × 3 mm. The UL94 vertical burning test was performed on a CFZ-2-type instrument (Jiangning Analysis Instrument Company, China) according to ASTM D 3801-2010, and the dimensions of each sample were 100 mm × 13 mm × 3 mm.

The cone calorimeter test was performed on a FTT2000 cone calorimeter instrument (UK) according to ISO5660-2002 standard under an external heat flux of 50 kW m^{-2}, and the dimensions of each specimen were 100 mm × 100 mm × 3 mm.

The thermo-gravimetric (TG) analysis was conducted on a SOTA-851 (Mettler-Toledo, Switzerland) instrument with a heating rate of 20 °C min^{-1}. About 5 mg sample

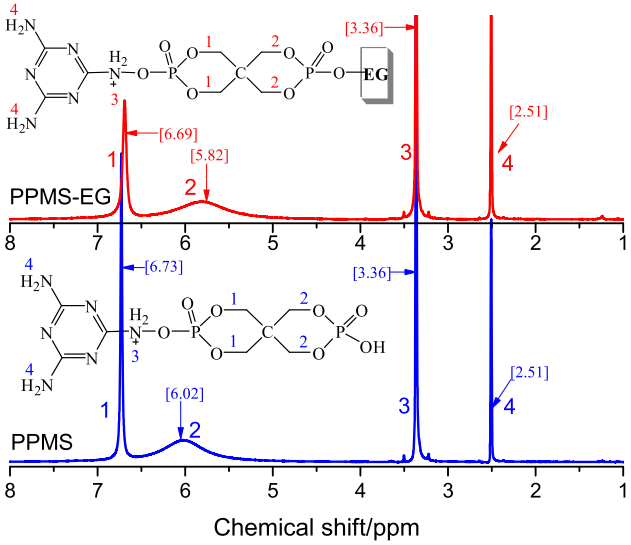

Fig. 2 ^{1}H NMR spectra of PPMS and PPMS-EG flame retardants

was heated from 25 to 800 °C under a nitrogen flow of 40 mL min^{-1}. The calculated residual masses (W_{cal}) were obtained from the following Eq. (1) [26].

$$W_{cal}(T) = \sum_{i=1}^{n} \chi_i W_i(T) \quad (1)$$

where χ_i is the content of compound i and W_i is the residual weight of compound i in the TG test.

X-ray photoelectron spectroscopy (XPS) of the char residues obtained after the cone calorimeter test was recorded on an ESCALAB 250Xi electron spectrometer (ThermoFisher-VG Scientific, USA).

Results and discussion

Characterization of PPMS and PPMS-EG

The structures of PPMS and PPMS-EG were examined by FTIR, ^{1}H NMR, and SEM–EDS (Figs. 1–3). The FTIR spectra of EG, PPMS, and PPMS-EG are shown in Fig. 1. For EG, the peaks at 3488, 1655, and 1118 cm^{-1} are assigned to the vibration of –OH groups, C=O groups, and C–O groups, respectively [27, 28], indicating the presence of C–OH groups in the structure of EG that can react with P–OH groups in PA. In the spectrum of PPMS, the characteristic peaks at 3392 and 3157 cm^{-1} (N–H groups), 2955 cm^{-1} (–CH_3 groups), 2852 cm^{-1} (–CH_2– groups), 2360 cm^{-1} (P–OH groups),1670 cm^{-1} (C=N groups), 1406 cm^{-1} (P–N groups), 1245 cm^{-1} (P=O groups), 1109 cm^{-1} (C–O–C groups), 1050 and 959 cm^{-1} (P–O–C groups) are found [10, 29, 30], indicative that the PPMS was successfully synthesized, as shown in Scheme1. In the spectrum of PPMS-EG, the major characteristic peaks appeared in both EG and PPMS are found, indicating that

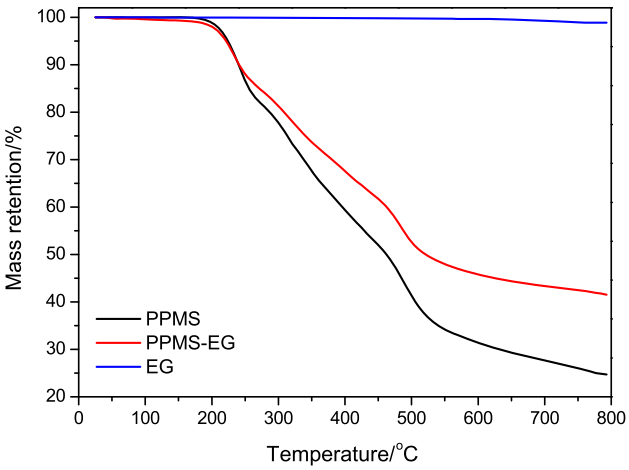

Fig. 4 TG curves of flame retardants under nitrogen atmosphere at a heating rate of 20 °C min^{-1}

PPMS was successfully grafted on the surface of EG, as shown in Scheme 2.

To further validate the structures of PPMS and PPMS-EG, ^{1}H NMR test was conducted, and the results are shown in Fig. 2. As shown in Fig. 2, the signal peaks of H atom at 6.73–6.69 ppm (–CH_2 in bicyclic phosphate adjacent to P–O–NH_2^+ group), 5.82–6.02 ppm (–CH_2 in bicyclic phosphate adjacent to P–OH group or P–O–EG group), 3.36 ppm (–NH_2^+–), and 2.51 ppm (–NH_2 in melamine ring) are observed in the spectrum of both PPMS and PPMS-EG. It is important to note that the chemical shifts of –CH_2 groups in bicyclic phosphate for PPMS-EG are lower than those of PPMS, further confirming that the PPMS was successfully grafted on the surface of EG.

SEM–EDS analysis was employed to analyze the morphologies and compositions of PPMS and PPMS-EG, and the results are presented in Fig. 3. It can be observed that the PPMS particles exhibit a relatively regular blocky

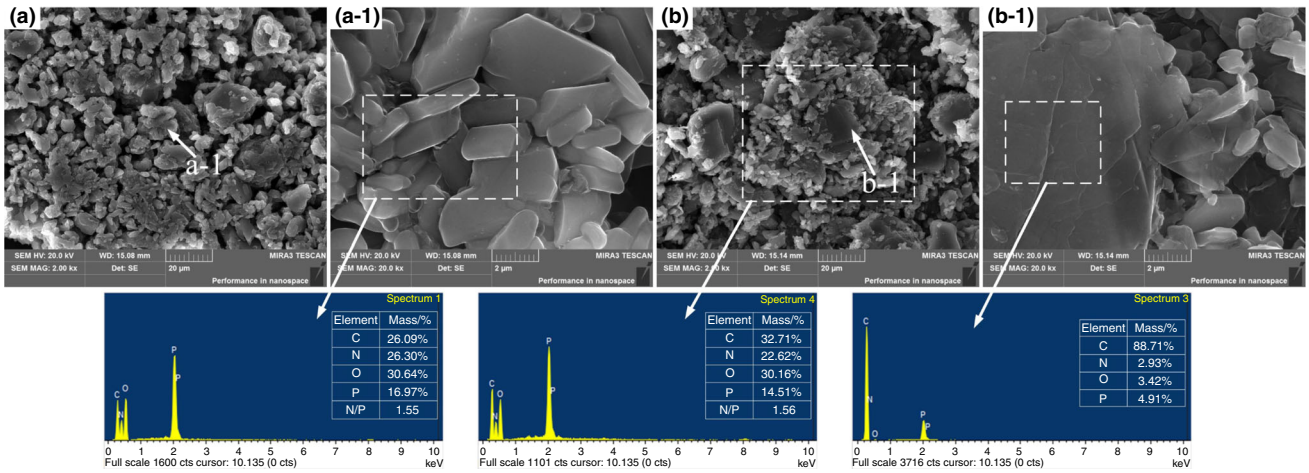

Fig. 3 SEM images and EDS maps of PPMS (**a**) and PPMS-EG (**b**) flame retardants

structure with the dimensions around several micrometers, while the PPMS-EG particles show uniform distribution of big plate-like structure surrounded by small blocky structure. In order to verify the chemical compositions of blocky structure and plate-like structure, the EDS mapping of the samples was taken, and the results are presented in Fig. 3. It can be seen that the plate-like structure in PPMS-EG mainly consists of carbon element (88.7 mass%), indicative that the plate-like structure is EG platelets. And, the distribution of N, O, and P elements on the surface of EG platelets reveals that intumescent flame retardant is grafted on the surface of EG platelets. Additionally, the mass ratio of nitrogen to phosphorus in both PPMS and PPMS-EG is approximately in accordance with the calculated content according to the chemical structure of PPMS. From the above results, it can be confirmed that PPMS and PPMS-EG flame retardants have been prepared successfully.

TG test was used to calculate the grafted PPMS content on the surface of EG by the thermal decomposition, and the results are shown in Fig. 4. As shown in Fig. 4, EG exhibits good thermal stability and remains 98.85 mass% residue at 800 °C. And, both PPMS and PPMS-EG exhibit three decomposition stages in the temperature ranges of 220–290 °C, 290–430 °C, and 430–800 °C, respectively. The first stage from 220 to 290 °C is ascribed to the scission of the phosphate ester bonds concomitant with the release of small molecules. The second stage in the range of 290–430 °C is assigned to the thermal decomposition of PPMS accompanying with the release of inert gases and intumescent char formation simultaneously. The third stage during 430–800 °C is ascribed to the degradation of unstable carbonized backbones, and the residual mass at 800 °C is 24.69 mass% for PPMS and 41.50 mass% for PPMS-EG. The content of PPMS on the surface of EG can be roughly calculated according to the equation [31]:

$$W_{\mathrm{PPMS}} = \frac{M_{\mathrm{EG}} - M_{\mathrm{PPMS-EG}}}{M_{\mathrm{EG}} - M_{\mathrm{PPMS}}} \quad (2)$$

where W_{PPMS} is the mass percentage of PPMS in PPMS-EG and M_{EG}, M_{PPMS}, and $M_{\mathrm{PPMS\text{-}EG}}$ are the mass losses of EG, PPMS, and PPMS-EG at 800 °C, respectively.

According to Eq. (2), the mass percentages of PPMS and EG in the PPMS-EG are estimated to be 77.33% and 22.67%, respectively.

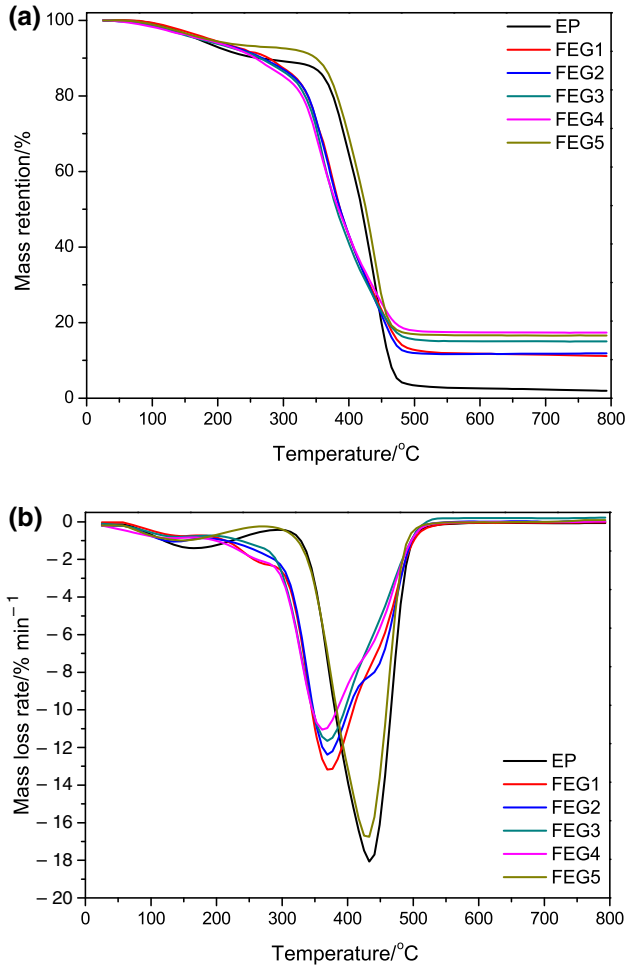

Fig. 5 TG (**a**) and DTG (**b**) curves of flame-retarded epoxy resins

Thermo-gravimetric analysis

The TG test was used to evaluate the thermal stability and char-forming ability of flame-retarded epoxy resins, and the corresponding curves are shown in Fig. 5. The related data, including, respectively, the onset decomposition temperature ($T_{5\%}$), defined as the 5% mass loss temperature, the $T_{\max}$, defined as the maximum mass loss rate temperature, the *PMLR*, defined as the maximum mass loss rate, the W_{exp}, defined as the experimental value of residual mass, the W_{cal}, defined as the calculated value of residual mass, and $\Delta W = W_{\mathrm{exp}} - W_{\mathrm{cal}}$, are listed in Table 2.

Under a nitrogen atmosphere, EP begins to decompose at 169.5 °C and leaves 1.9 mass% residue at 800 °C, as shown in Fig. 5. The thermal decomposition process of EP occurs in two stages ranging from 65 to 300 and from 300 to 500 °C, respectively, where the second stage is the dominated one with 85.8% mass loss. With the incorporation of PPMS or PPMS-EG, the TG curves of samples show two decomposition stages in the temperature ranges of 65–200 °C and 200–500 °C, respectively, and the second stage is the dominated one. The $T_{5\%}$ of FEG1–FEG4 is obvious above that of EP, indicating an enhancement in the thermal stability. In addition, the *PMLR* values of FEG1–FEG4 are 27.1, 31.5, 35.9, and 39.2% lower, respectively, than those of EP, resulting in a positive effect on the char forming. Moreover, the W_{exp} values at 800 °C for FEG1–FEG4 are higher than the corresponding W_{cal} values at 800 °C, indicating an enhancement in the char-forming

Table 2 TG results for flame-retarded epoxy resins under a nitrogen atmosphere at a heating rate of 20 °C min^{-1}

Samples	$T_{5\%}$/°C	T_{max}/°C	*PMLR*/% min^{-1}	W_{exp} at 800 °C/%	W_{cal} at 800 °C/%	ΔW at 800 °C/%
EP	169.5	433.2	18.1	1.9	–	–
FEG1	188.7	369.3	13.2	11.1	5.4	5.7
FEG2	175.5	368.9	12.4	11.9	5.9	6.0
FEG3	176.5	369.1	11.6	15.1	7.9	7.2
FEG4	178.9	368.5	11.0	17.4	9.9	7.5
FEG5	184.6	433.3	16.7	16.6	16.5	0.1

ability. ΔW can be used to describe this char-forming ability, and a higher ΔW value of the sample corresponds a higher char-forming ability, as supported by Si [32]. Compared to FEG1 with 15 mass% PPMS, FEG3 with 15 mass% PPMS-EG shows a higher ΔW value at 800 °C, indicating that PPMS-EG has better char-forming ability in the EP matrix. With the incorporation of EG, it clearly indicates that the thermal degradation process of FEG5 is similar to EP, and the W_{exp} value at 800 °C of FEG5 is close to the W_{cal} value at 800 °C. This result indicates that EG only acts as an inert filler in the matrix and cannot promote the charring of EP matrix, and the increased thermal stability of composites is ascribed to the fact that EG can provide an effective insulating layer against the heat and mass transfer. Therefore, the sample with EG has different thermal behavior compared to the sample with either PPMS or PPMS-EG.

As shown in Table 2, it is noted that the thermal stability and char-forming ability of the flame-retarded EPs are dependent on the type and amount of flame retardants. When the same amount of flame retardants is added, PPMS-EG shows better charring effect in the EP matrix than that of either PPMS or EG, thus greatly decreasing the mass loss rate and yielding more carbonaceous char components in the condensed phase. In addition, as PPMS-EG is added into EP matrix, the mass loss rate and *PMLR* of the samples are gradually decreased with increasing content of PPMS-EG concomitant with the increase in the T_d and residual mass. For example, the W_{exp} values at 800 °C of the samples with 10, 15, and 20 mass% PPMS-EG are 11.9, 15.1, and 17.4 mass%, respectively. Based on the above results, it can be concluded that the incorporation of PPMS-EG imparts well char-forming effect in the EP matrix compared to that of either PPMS or EG, thus leading to the formation of more char layer to slow down the mass loss rate of polymer and impede mass and heat transfer in the pyrolysis process.

LOI and UL94 tests

LOI and UL94 tests were applied to assess the flame retardancy of the EP composites, and the corresponding

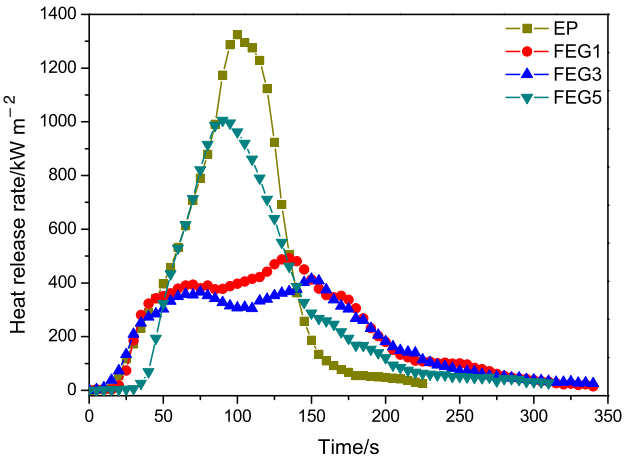

Fig. 6 Heat release rate curves of flame-retarded epoxy resins at a heat flux of 50 kW m^{-2}

results are summarized in Table 1. As shown in Table 1, the incorporation of flame retardants enhances the flame retardancy of EP materials. In detail, the LOI value of EP is 19.2% and is failed to pass the UL94 test. With the incorporation of PPMS-EG, the LOI value and UL94 rating of the EP composites are gradually improved with increasing PPMS-EG content, and FEG4 with 20 mass% PPMS-EG acquires the highest of LOI value (27.3%) and passes UL94 V-0 rating. In addition, the same loading of PPMS-EG imparts higher LOI value and UL94 rating to EP matrix than those of either PPMS or EG. This phenomenon can be explained by the high char-forming ability of PPMS-EG in EP matrix, as confirmed by TG test. Generally, the high char-forming ability helps to form more char residue on the surface of material that insulates the transfer of heat and mass between flame and underlying material, thus effectively retarding the combustion process. Therefore, the sample with PPMS-EG possesses a better flame retardancy in comparison with the sample with the same loading of PPMS or EG separately. In addition, it should be noted that FEG5 with a UL94 HB rating has a higher LOI value than FEG1 with a UL94 V-2 rating. This result can be ascribed to the differences in burning condition between LOI and UL94 tests as well as the flame-retardant actions

Table 3 Cone calorimeter data for flame-retarded epoxy resins at a heat flux of 50 kW m^{-2}

Samples	PHRR/kW m^{-2}	THR/MJ m^{-2}	PSPR/m^2 s^{-1}	TSR/m^2 m^{-2}	Residue/%
EP	1324.6	95.7	0.136	1276.4	4.2
FEG1	491.6	74.0	0.079	1030.6	21.1
FEG3	414.3	66.7	0.073	977.2	27.5
FEG5	1015.3	85.3	0.103	1142.9	15.2

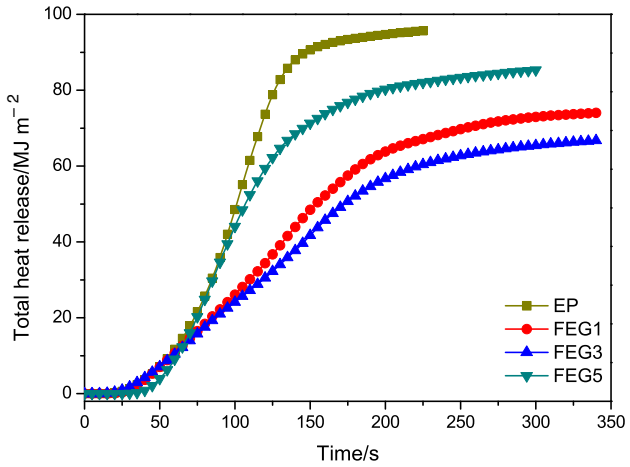

Fig. 7 Total heat release curves of flame-retarded epoxy resins at a heat flux of 50 kW m^{-2}

between PPMS and EG [33]. For example, the loose char residue of FEG5 with EG is easily blown away during burning [17], which helps to accelerate the heat away from the preheating part and then improve the LOI value. But, the dropping char with high temperature is easily to ignite the cotton, resulting in failing to classify the UL94 test.

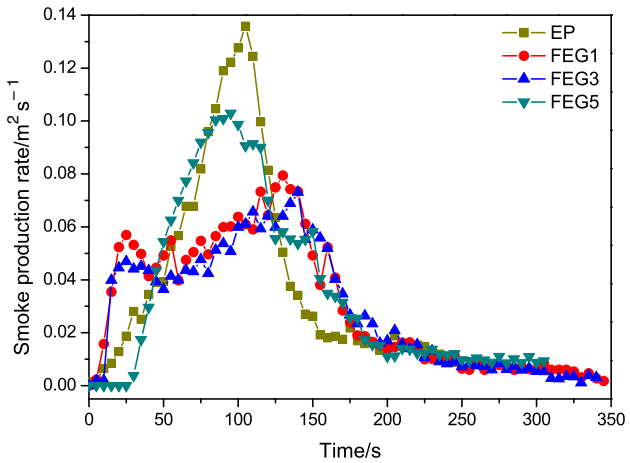

Fig. 8 Smoke production rate curves of flame-retarded epoxy resins at a heat flux of 50 kW m^{-2}

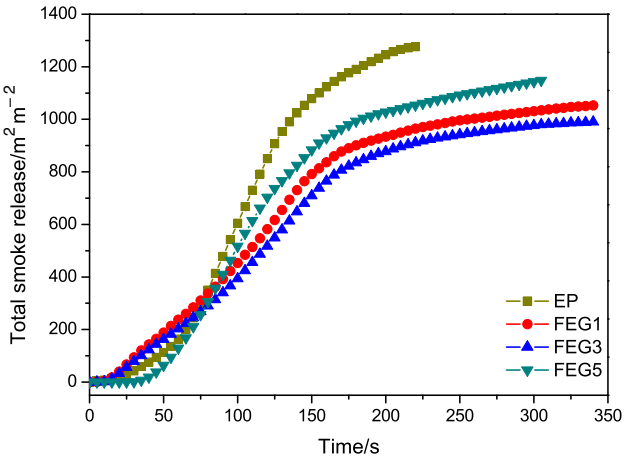

Fig. 9 Total smoke release curves of flame-retarded epoxy resins at a heat flux of 50 kW m^{-2}

Cone calorimeter test

To evaluate the combustion behaviors of flame-retarded EPs in reality, the cone calorimeter test was employed and the results are presented in Figs. 6–9 and Table 3, respectively. As shown in Figs. 6 and 7, EP burns quickly after ignition with a single peak heat release rate (PHRR) of 1324.6 kW m^{-2} at 100 s, accompanying with a high total heat release (THR) of 95.7 MJ m^{-2} after burning. By comparing with EP, the incorporation of flame retardants greatly decreases the PHRR and THR of the EP composites, indicating the enhancement of flame retardancy. In detail, the PHRR and THR values of the EP composites are reduced by 62.9% and 22.7% for FEG1, 68.7% and 30.3% for FEG3, 23.4% and 10.9% for FEG5, respectively. In particular, FEG3 with PPMS-EG shows the lowest PHRR and THR values among the samples, corresponding to the best flame retardancy. The increased flame retardancy can be ascribed to that the flame retardants generate an insulating layer that segregates the heat and mass transfer during burning. For the sample with PPMS or PPMS-EG, two peaks are found in HRR curve, and the first HRR peak is ascribed to the formation of an effective intumescent char, and then, the thermal degradation and cracking of intumescent char at high temperature results in another HRR peak. However, the sample with EG shows a similar single sharp peak in HRR from that of EP, indicating that EG only acts as a physical barrier to reduce the burning

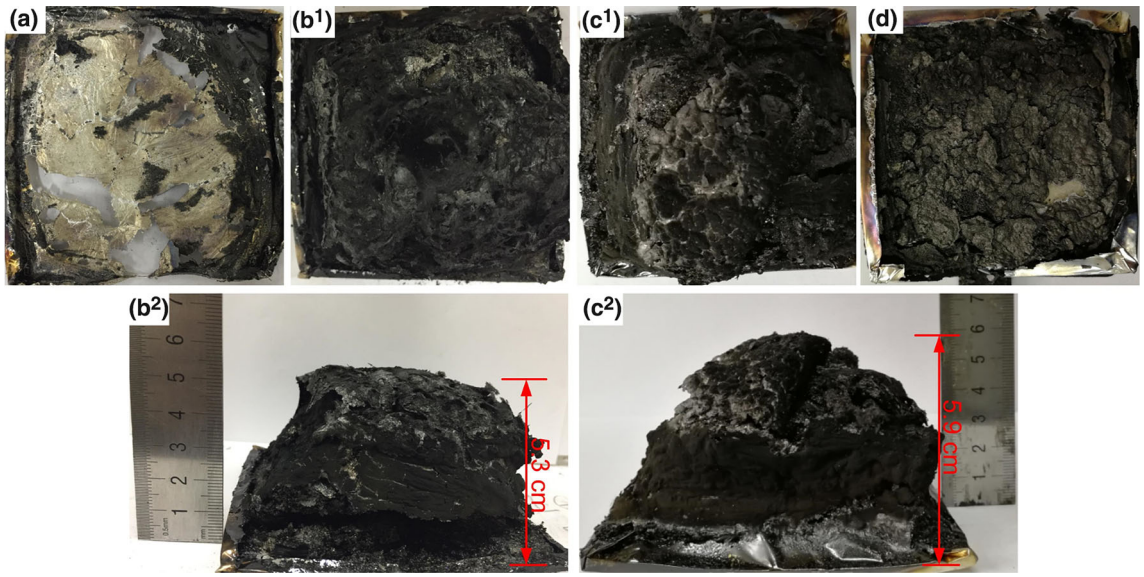

Fig. 10 Digital photographs of the char residues of EP (**a**), FEG1 (**b**), FEG3 (**c**), and FEG5 (**d**) obtained after cone calorimeter test; superscript 1 represents the top view, and 2 represents the side view

intensity of EP matrix and hardly affects the flaming behavior of EP, as supported by TG test. Thus, EG exhibits a lower flame retardant efficiency in EP matrix than that of either PPMS-EG or PPMS. But, the introduction of EG into intumescent system is beneficial to enhance the barrier effect and thermal stability of intumescent char [20], thus effectively preventing the underlying materials from further combustion. This illustrates the combination of PPMS and EG by chemical bonding imparts excellent synergistic flame retardant effect on the decreasing of HRR and THR in EP materials.

The smoke production rate (SPR) and total smoke release (TSR) curves of flame-retarded EPs are presented in Figs. 8 and 9, respectively. It is clearly seen that EP has a single peak SPR (PSPR) of 0.136 m^2 s^{-1}, and its TSR value reaches to 1276.4 m^2 m^{-2}. With the incorporation of flame retardants, the SPR and TSR values of the samples are greatly decreased from those of EP, indicative the enhancement of smoke suppression properties. In particular, the same addition of PPMS-EG possesses the lowest PSPR and TSR in the EP matrix, the next is PPMS, and the last is EG. In detail, the PSPR and TSR of FEG3 with

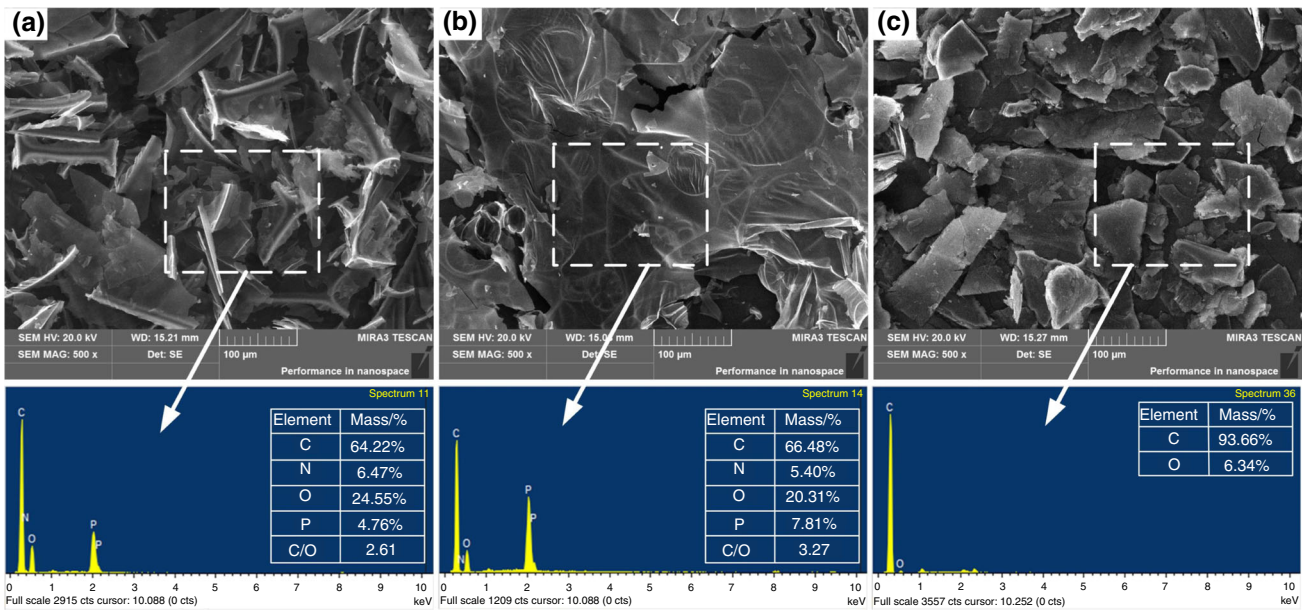

Fig. 11 SEM images and EDS maps of the char residues of FEG1 (**a**), FEG3 (**b**), and FEG (5) obtained after the cone calorimeter test

PPMS-EG are reduced by 46.3% for PSPR and 23.4% for TSR compared to those of EP. This result is mainly because of the fact that the super char-forming ability of PPMS-EG can promote the generation of a more compact char to segregate heat and mass transfer, thus resulting in high mass retention after burning, as listed in Table 3. And, the high mass retention is beneficial to reduce the release of flammable gases and smoke precursors during burning, thus exhibiting good smoke suppression properties. Taking all into consideration, PPMS-EG performs better in enhancing the flame-retardant and smoke suppression properties of EP materials than either PPMS or EG.

Morphology and chemical structure of char residues

The digital photographs of the char residues obtained after the cone calorimeter test are shown in Fig. 10. It can be seen that EP has hardly any residue left after burning, while the samples with flame retardants leave a considerable volume of char residues to prevent the underlying materials from burning. In detail, FEG5 with EG leaves a very loose and thin char layer without intumescence, while FEG1 and FEG3 form a compact and intumescent char layer. Compared to FEG1 with PPMS, the char layer of FEG3 with PPMS-EG is more compact and intumescent without obvious cracks and holes on the surface, thus exhibiting better barrier effect on the reducing of heat and smoke release during burning. It is further testified that PPMS-EG imparts excellent flame-retardant and smoke suppression effects in EP materials.

The SEM images and EDS maps of the char residues after the cone calorimeter test are presented in Fig. 11. The SEM images further illustrate that the FEG3 with PPMS-EG tends to form a more compact and continuous char residue with less voids and cracks than that of FEG1 and FEG5, coinciding with the highest flame-retardant and smoke suppression efficiency among the samples. Obviously, the combination of PPMS and EG by chemical bonding can lead to the adhesion between phosphorus-rich residue and expanded graphite plates and thus forms a well protective-effect char residue. By comparing the elemental composition and content of char residues, it can be seen that FEG5 is merely composed of EG platelets, further demonstrating that EG only acts as a thermal barrier to reduce the combustion intensity of EP rather than change the combustion behavior of EP matrix. Compared to FEG1, the char residue of FEG3 has higher carbon and phosphorus contents, indicating that more phosphorus-rich aromatization structures remained in the condensed phase. In addition, the corresponding C/O ratio of char residue is increased to 3.27 in FEG3 from that of 2.61 in FEG1, and the increased C/O ratio tends to endow the char residue with high antioxidation property and denser structure [19, 30]. As a result, the same addition of PPMS-EG in EP matrix can form a more thermally stable barrier to decrease the combustion intensity, thus effectively improving the fire safety of EP system.

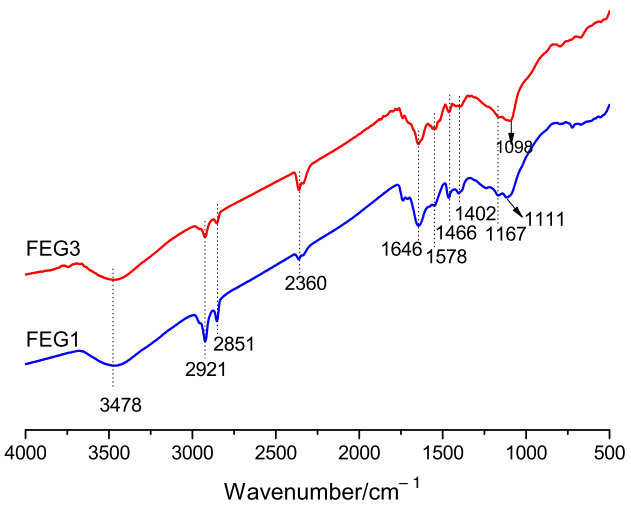

Fig. 12 FTIR spectra of the char residues of FEG1 and FEG3 obtained from the cone calorimeter test

FTIR test was conducted to determine the functional groups of the char residues obtained after the cone calorimeter test, and the corresponding results are presented in Fig. 12. The similar characteristic peaks at 3478 cm^{-1} (N–H and –OH groups), 2921 and 2851 cm^{-1} (–CH_2– and –CH– groups), 2360 cm^{-1} (O–H in O=P–OH group), 1646 cm^{-1} (C=C and C=N group), 1466 cm^{-1} (C–C in aromatic ring), 1402 cm^{-1} (P–N group), and 1167 cm^{-1} (PO_2/PO_3) are observed in both FEG1 and FEG3 [34–36]. In addition, FEG1 shows a strong peak at 1111 cm^{-1} that can be assigned to the vibration of C–O–C, P–O–P, and P–O–C groups [20, 37]. The redshift of P–O–C, P–O–P, and C–O–C groups to 1098 cm^{-1} is visible in the spectra of FEG3 due to the interaction between EG platelets and P-containing cross-linking structures in the residue. Additionally, the peak intensity at 1578 cm^{-1} (polyaromatic species) for FEG3 is obviously stronger and broader than that of FEG1 [38], which is beneficial to form more aromatic char.

Table 4 XPS results of the char residues of FEG1 and FEG3 after the cone calorimeter test

Samples	C/at%	O/at%	N/at%	P/at%	O/C	N/C	P/C
FEG1	77.31	16.57	3.86	2.26	0.21	0.050	0.029
FEG3	61.45	28.38	3.42	6.74	0.46	0.056	0.11

The chemical structure and atomic concentration of the char residues after the cone calorimeter test were further analyzed by XPS, and the detailed composition is listed in Table 4. For FEG3, it has much higher values of O/C, N/C, and P/C than those of FEG1, especially for the P/C value. This result indicates that functionalized EG with PPMS can remain more cross-linking structures containing P, N, and O element in the char residue. Generally, more cross-linking structures remained in the condensed phase are beneficial for the formation of a more compact and intumescent char layer [39], which give an explanation of the high-quality char obtained from FEG3.

High resolutions of C_{1s}, N_{1s}, O_{1s}, and P_{2p} spectrums of FEG1 and FEG3 are depicted in Fig. 13. In the C_{1s} spectrum, the peaks at 284.5, 285.0, and 286.3 eV can be assigned to the C–H/C–C in the aliphatic and aromatic species in char, C–O–C/C–OH/C–N/C–O–P groups, and C=C/C=O/C=N groups, respectively [40]. Interestingly, the relative contents of the bonds at 285.0 eV for FEG3 are obvious higher than those of FEG1, indicating that the same addition of PPMS-EG forms more cross-linking structures containing C–O or C–N. In the N_{1s} spectrum, the bands at 398.7, 400.2, and 402.1 eV are assigned to C=N in triazine rings, C–N groups, and N–H groups, respectively [41], while the peak intensities at 400.2 eV for FEG3 increase compared to FEG1, indicating that more cross-linking structures containing C–N are formed. In the O_{1s} spectrum, two peaks appear at 531.6 and 533.1 eV, wherein the former is assigned to the C=O or P=O groups in phosphate and carbonyl compounds, and the latter is ascribed to the –O– bond in P–O–C or P–O–P or C–O groups [42]. It is apparent that the relative ratio of –O– bonds in total O for FEG3 is higher than that of FEG1, implying more O-containing cross-linking structures remained in the char residue that can be proved by C_{1s} XPS spectra. In Fig. 13 d, the spectra of P_{2p} exhibit two bands at 134.0 and 134.6 eV that can be assigned to the P–O/PO_3 groups in phosphate and P–O–C group, respectively [40]. It

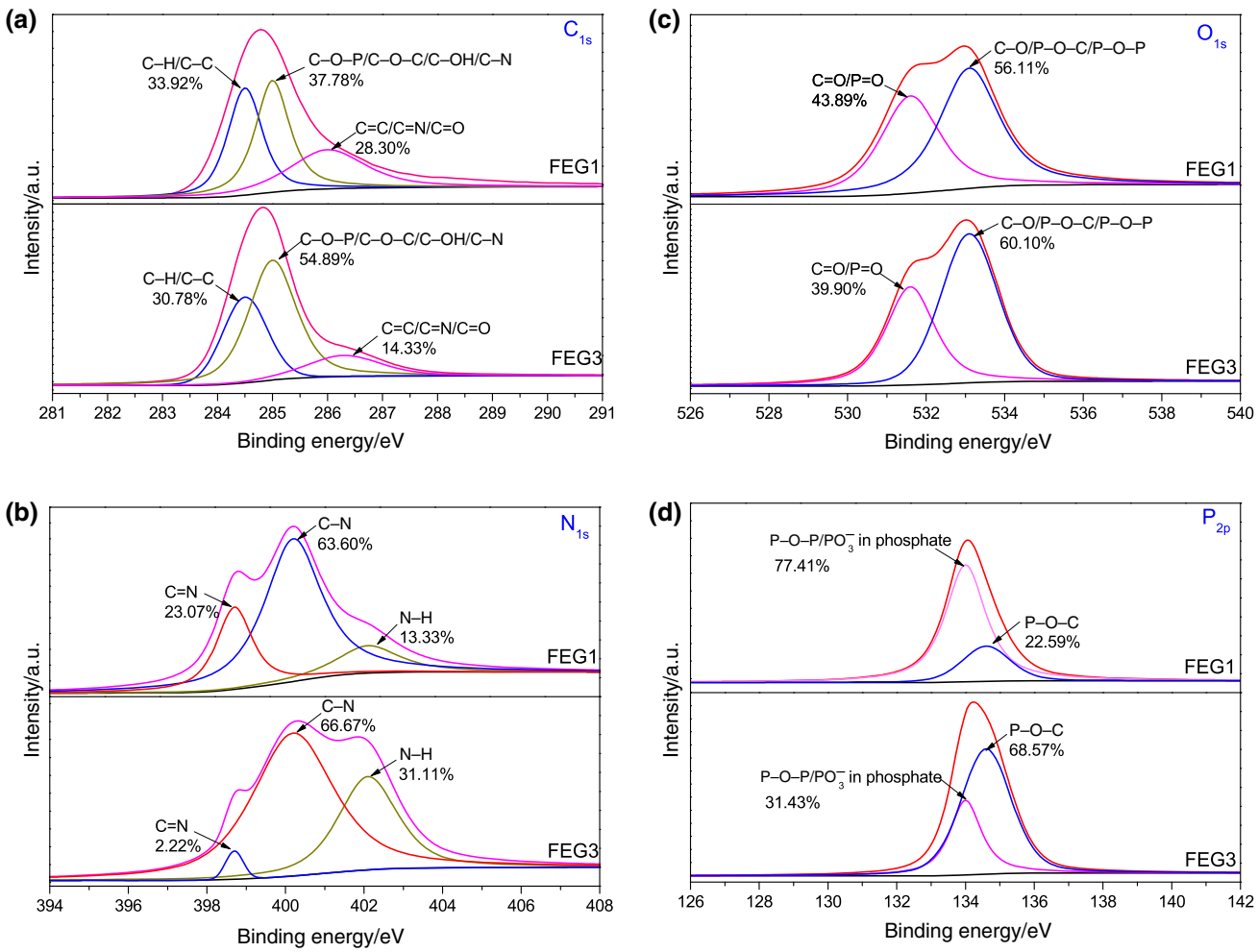

Fig. 13 High-resolutions of (**a**) C_{1s} (**b**) N_{1s}, (**c**) O_{1s}, and (**d**) P_{2p} XPS spectra of the char residue of FEG1 and FEG3 obtained after the cone calorimeter test

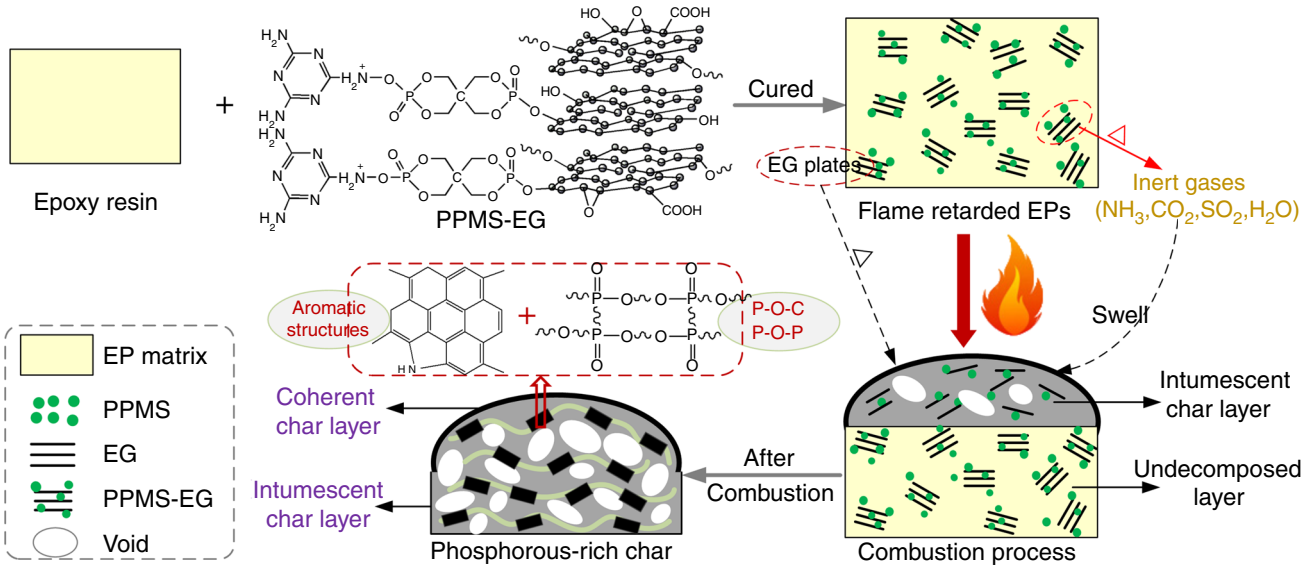

Scheme 3 Possible flame-retardant and smoke suppression mechanism of PPMS-EG in EP matrix

is noted that the relative content of P–O–C bond for FEG3 increases to 68.57% from that of 22.59% in FEG1, indicating that more cross-linking structures are formed, as confirmed by the results of C_{1s} and O_{1s} spectra. These results verify that the incorporation of PPMS-EG is beneficial to form more cross-linking structures containing P–O–C, P–O–P, C–N, and C–O–C groups that endow better barrier effect and antioxidation property to the resulting char, thus effectively insulating the heat and mass transfer between the gas and condensed phases (Fig. 13).

Based on the discussion above, it is reasonable to demonstrate that the combination of PPMS and EG by chemical bonding contributes to form more cross-linking structures in the condensed phase that provide a compact and intumescent char against the release of heat and smoke, thus producing excellent flame-retardant and smoke suppression efficiencies in EP matrix. And, the possible flame-retardant and smoke suppression mechanism of PPMS-EG in EP matrix is presented in Scheme 3.

Conclusions

In this work, a novel mono-component intumescent flame retardant, pentaerythritol phosphate melamine salt (PPMS)-functionalized expandable graphite (PPMS-EG), was synthesized via chemical grafting PPMS on the surface of EG. The chemical structure, morphology, and thermal property of PPMS-EG were carefully characterized by various analytical instruments. The FTIR, ^{1}H NMR, and SEM–EDS analyses verified that the PPMS was successfully grafted on the surface of EG platelets, and the percentage of PPMS in PPMS-EG was 77.33%, as calculated by TG test. The results of LOI and UL94 show that the incorporation of PPMS-EG improves the flame retardancy of EP composites, and FEG4 with 20 mass% PPMS-EG passes the UL94 V-0 rating and the LOI reaches 27.3%. Cone calorimeter test shows that the same addition of PPMS-EG reduces the PHRR, THR, SPR, and TSR values of epoxy resin more efficiently than that of either PPMS or EG, revealing the higher flame-retardant and smoke suppression efficiencies. TG test shows that the addition of PPMS-EG changes the thermal degradation behavior of EP matrix concomitant with the increase in the $T_{5\%}$, residual mass, and ΔW, implying the enhancement of thermal stability and char-forming ability. Morphological analysis of the char residue shows that the incorporation of PPMS-EG into EP matrix generates a more compact and intumescent char to retard the heat and smoke release, thus effectively preventing the internal material from further burning. FTIR and XPS analyses reveal that the incorporation of PPMS-EG positively contributes to the formation of more phosphorus-rich cross-linking char and aromatic char in condensed phase, thus providing a well protective-effect char layer.

Acknowledgements This work was supported by the National Natural Science Foundation of China (No. 51676210), the Hunan Provincial Natural Science Foundation of China (No. 2018JJ3668), the Postdoctoral Science Foundation of Central South University, and the Project funded by China Postdoctoral Science Foundation (No. 2017M612587).

References

1. Sut A, Greiser S, Jäger C, Schartel B. Synergy in flame-retarded epoxy resin. J Therm Anal Calorim. 2017;128(1):141–53.

2. Qiu S, Wang X, Yu B, Feng X, Mu X, Yuen RKK, Hu Y. Flame-retardant-wrapped polyphosphazene nanotubes: a novel strategy for enhancing the flame retardancy and smoke toxicity suppression of epoxy resins. J Hazard Mater. 2017;325:327–39.
3. Wang X, Hu Y, Song L, Xing W, Lu H, Lv P, Jie G. Flame retardancy and thermal degradation mechanism of epoxy resin composites based on a DOPO substituted organophosphorus oligomer. Polymer. 2010;51:2435–45.
4. Khalili P, Tshai KY, Hui D, Kong I. Synergistic of ammonium polyphosphate and alumina trihydrate as fire retardants for natural fiber reinforced epoxy composite. Compos Part B Eng. 2017;114:101–10.
5. Jiao C, Zhang C, Dong J, Chen X, Qian Y, Li S. Combustion behavior and thermal pyrolysis kinetics of flame-retardant epoxy composites based on organic-inorganic intumescent flame retardant. J Therm Anal Calorim. 2015;119:1759–67.
6. Bourbigot S, Le Bras M, Duquesne S, Rochery M. Recent advances for intumescent polymers. Macromol Mater Eng. 2004;289:499–511.
7. Zhao X, Gao S, Liu G. A THEIC-based polyphosphate melamine intumescent flame retardant and its flame retardancy properties for polylactide. J Anal Appl Pyrol. 2016;122:24–34.
8. Zhang F, Sun W, Wang Y, Liu B. Influence of the pentaerythritol phosphate melamine salt content on the combustion and thermal decomposition process of intumescent flame-retardant ethylene-vinyl acetate copolymer composites. J Appl Polym Sci. 2015;132:42148.
9. Makhlouf G, Hassan M, Nour M, Abdel-Monem YK, Abdelkhalik A. Evaluation of fire performance of linear low-density polyethylene containing novel intumescent flame retardant. J Therm Anal Calorim. 2017;130:1031–41.
10. Zhang P, He Y, Tian S, Fan H, Chen Y, Yan J. Flame retardancy, mechanical, and thermal properties of waterborne polyurethane conjugated with a novel phosphorous-nitrogen intumescent flame retardant. Polym Compos. 2017;38:452–62.
11. Tang M, Qi F, Chen M, Sun Z, Xu Y, Chen X, Zhang Z, Shen R. Synergistic effects of ammonium polyphosphate and red phosphorus with expandable graphite on flammability and thermal properties of HDPE/EVA blends. Polym Advan Technol. 2016;27:52–60.
12. Alongi J, Han Z, Bourbigot S. Intumescence: tradition versus novelty. A comprehensive review. Prog Polym Sci. 2015;51:28–73.
13. Wang X, Kalali EN, Wan J, Wang D. Carbon-family materials for flame retardant polymeric materials. Prog Polym Sci. 2017;69:22–46.
14. Li Y, Zou J, Zhou S, Chen Y, Zou H, Liang M, Luo W. Effect of expandable graphite particle size on the flame retardant, mechanical, and thermal properties of water-blown semi-rigid polyurethane foam. J Appl Polym Sci. 2014;131(3):1082–90.
15. Luo W, Li Y, Zou H, Liang M. Study of different-sized sulfur-free expandable graphite on morphology and properties of water-blown semi-rigid polyurethane foams. RSC Adv. 2014;4:37302–10.
16. Laachachi A, Burger N, Apaydin K, Sonnier R, Ferriol M. Is expanded graphite acting as flame retardant in epoxy resin? Polym Degrad Stabil. 2015;117:22–9.
17. Yang S, Wang J, Huo S, Wang M, Wang J, Zhang B. Synergistic flame-retardant effect of expandable graphite and phosphorus-containing compounds for epoxy resin: strong bonding of different carbon residues. Polym Degrad Stabil. 2016;128:89–98.
18. Wang N, Xu G, Wu Y, Zhang J, Hu L, Luan H, Fang Q. The influence of expandable graphite on double-layered microcapsules in intumescent flame-retardant natural rubber composites. J Therm Anal Calorim. 2016;123:1239–51.
19. Xi W, Qian L, Huang Z, Cao Y, Li L. Continuous flame-retardant actions of two phosphate esters with expandable graphite in rigid polyurethane foams. Polym Degrad Stabil. 2016;130:97–102.
20. Zheng Z, Liu Y, Zhang L, Wang H. Synergistic effect of expandable graphite and intumescent flame retardants on the flame retardancy and thermal stability of polypropylene. J Mater Sci. 2016;51:5857–71.
21. Liu Y, He J, Yang R. Effects of Dimethyl Methylphosphonate, Aluminum hydroxide, ammonium polyphosphate, and expandable graphite on the flame retardancy and thermal properties of polyisocyanurate-polyurethane foams. Ind Eng Chem Res. 2015;54:5876–84.
22. Zhu H, Zhu Q, Li J, Tao K, Xue L, Yan Q. Synergistic effect between expandable graphite and ammonium polyphosphate on flame retarded polylactide. Polym Degrad Stabil. 2011;96:183–9.
23. Han J, Liang G, Gu A, Ye J, Zhang Z, Yuan L. A novel inorganic-organic hybridized intumescent flame retardant and its super flame retarding cyanate ester resins. J Mater Chem A. 2013;1:2169–82.
24. Chen X, Zhuo J, Song W, Jiao C, Qian Y, Li S. Flame retardant effects of organic inorganic hybrid intumescent flame retardant based on expandable graphite in silicone rubber composites. Polym Adv Technol. 2014;25:1530–7.
25. Liu D, Zhong X, Shi X, Qi Y, Zhu T, Shao M, Zhang F. Pentaerythritol phosphate melamine salt, a new aggregating reagent for oilfield chemical sand control: preparation, properties, and mechanism. Energy Fuel. 2016;30:2503–13.
26. Fontaine G, Bourbigot S, Duquesne S. Neutralized flame retardant phosphorus agent: facile synthesis, reaction to fire in PP and synergy with zinc borate. Polym Degrad Stabil. 2008;93(1):68–76.
27. Wang G, Yang J. Influences of expandable graphite modified by polyethylene glycol on fire protection of waterborne intumescent fire resistive coating. Surf Coat Technol. 2010;204:3599–605.
28. Huang G, Chen S, Tang S, Gao J. A novel intumescent flame retardant-functionalized graphene: nanocomposite synthesis, characterization, and flammability properties. Mater Chem Phys. 2012;135:938–47.
29. Wang P, Yang F, Cai Z. Synergistic effect of organo-montmorillonite and DOPO-based oligomer on improving the flame retardancy of epoxy thermoset. J Therm Anal Calorim. 2017;128:1429–41.
30. Yan L, Xu Z, Wang X. Influence of nano-silica on the flame retardancy and smoke suppression properties of transparent intumescent fire-retardant coatings. Prog Org Coat. 2017;112:319–29.
31. Ye L, Meng X, Ji X, Li Z, Tang J. Synthesis and characterization of expandable graphite-poly(methyl methacrylate) composite particles and their application to flame retardation of rigid polyurethane foams. Polym Degrad Stabil. 2009;94:971–9.
32. Si M, Feng J, Hao J, Xu L, Du J. Synergistic flame retardant effects and mechanisms of nano-Sb_2O_3 in combination with aluminum phosphinate in poly(ethylene terephthalate). Polym Degrad Stabil. 2014;100:70–8.
33. Xu Z, Yan L, Liu D, Ni T, Peng J, Xu Y. Correlations between measurements of flame-retarded high-density polyethylene composites subjected to three conventional fire tests. In: Harada K, Matsuyama K, Himoto K, Nakamura Y, Wakatsuki K, editors. Fire science and technology 2015. Singapore: Springer; 2017. p. 599–607.
34. Yang A, Deng C, Chen H, Wei Y, Wang Y. A novel Schiff-base polyphosphate ester: highly-efficient flame retardant for polyurethane elastomer. Polym Degrad Stabil. 2017;144:70–82.
35. Shi Y, Yu B, Zheng Y, Guo J, Chen B, Pan Z, Hu Y. A combination of POSS and polyphosphazene for reducing fire hazards of epoxy resin. Polym Adv Technol. 2018;29(4):1242–54.

36. Li H, Hu Z, Zhang S, Gu X, Wang H, Jiang P, Zhao Q. Effects of titanium dioxide on the flammability and char formation of water-based coatings containing intumescent flame retardants. Prog Org Coat. 2015;78:318–24.
37. Xu Z, Chu Z, Yan L. Enhancing the flame-retardant and smoke suppression properties of transparent intumescent fire-retardant coatings by introducing boric acid as synergistic agent. J Therm Anal Calorim. 2018;133:1241–1252.
38. Murat Unlu S, Tayfun U, Yildirim B, Dogan M. Effect of boron compounds on fire protection properties of epoxy based intumescent coating. Fire Mater. 2017;41(1):17–28.
39. Yan L, Xu Z, Wang X. Synergistic effects of organically modified montmorillonite on the flame-retardant and smoke suppression properties of transparent intumescent fire-retardant coatings. Prog Org Coat. 2018;122:107–18.
40. Guan Y, Huang J, Yang J, Shao Z, Wang Y. An effective way to flame-retard biocomposite with ethanolamine modified ammonium polyphosphate and its flame retardant mechanisms. Ind Eng Chem Res. 2015;54:3524–31.
41. Yuan B, Fan A, Yang M, Chen X, Hu Y, Bao C, Jiang S, Niu Y, Zhang Y, He S, Dai H. The effects of graphene on the flammability and fire behavior of intumescent flame retardant polypropylene composites at different flame scenarios. Polym Degrad Stabil. 2017;143:42–56.
42. Wang P, Xia L, Jian R, Ai Y, Zheng X, Chen G, Wang J. Flame-retarding epoxy resin with an efficient P/N/S-containing flame retardant: preparation, thermal stability, and flame retardance. Polym Degrad Stabil. 2018;149:69–77.